Techno Science Africana Journal **Ibrahim**
Volume 6 Number 1 June, 2011 pp 99 - 107
ISSN 2006 - 2273

VALIDATION OF INDUCTION MOTOR PERFORMANCE OBTAINED FROM THE FINITE ELEMENT METHOD

S.B. Ibrahim
Department of Electrical Engineering, Bayero University, Kano

ABSTRACT

Performance characteristics of induction motor are traditionally predicted using analytical methods (i.e., equivalent circuit approach) with some approximations to the circuit parameters of the motor to allow for the effect of saturation. This technique usually gives acceptable, but not very accurate predictions of torque and current performances of the induction motor. In addition, the technique does not give information on the flux distribution pattern in the motor. This paper describes a numerical approach which overcomes these deficiencies through the use of a two-dimensional, nonlinear Finite Element Method (FEM) for excitation from a constant voltage source. The software used in this work is called "Finite Element Method Magnetics (FEMM)". The method uses combine finite element model for the rotor and stator, consisting of one-pole section of the induction motor. The use of this minimal model led to a fast execution time for the analysis. Comparison of stator current and torque for no-load and full-load conditions of the induction motor show good agreement with the operating data supplied by the manufacturer of the induction motor as well as the predictions obtained from the conventional constant parameter model (CCPM). In the course of this work, it has been assumed that the core losses, harmonic effects and the effect of rotor skewness in the induction motor under analysis are negligible. However, it is worthwhile to note that higher harmonics can create harmonic torques and losses in the induction motor that are not anticipated in this work.

KEYWORDS: ***Validation, Finite element method*, performance, *induction motor, conventional, Finite element method magnetics***

INTRODUCTION

Analysis and prediction of induction machines magnetic field pattern and characteristics are difficult due to the irregular geometry and non-linear magnetic material associated with the machine. The machine may be of the squirrel-cage or wound rotor type construction. In order to obtain accurately the performance of this machine, the magnetic field mapping of the internal structure is necessary.

This in turn, has necessitated the development of accurate methods for predicting the performance characteristics of these machines during the design stage. Examples of these performance indicators are open circuit characteristic, dynamic performance of the induction machine under load, dynamic performance under fault conditions and air gap flux distribution etc. In order to evaluate these performance quantities with precision, accurate and detail prediction of the electromagnetic field must be carried out under various operating conditions [1-6].

Classical analysis methods and analog techniques for induction machines have proved unsatisfactory except for simplified geometrical structures and boundary conditions [7]. Therefore, the need for numerical solution is recognized even in the early stages of the design art.

The rapid increase in computing power available to engineers and researchers as well as the advent of computer graphics has driven the development of electromagnetic finite element analysis (FEA). Finite element analysis is now being used to solve electrical machine problems such as the issue of losses, noise and greater harmonic content in the power supply [8].

Finite element field analysis offers the opportunity to perform detailed field calculations in regions which have complex shapes and which contain nonlinear magnetic materials. It is hardly surprising that the last three decades have seen numerous proposals for the use of finite elements for the analysis of electrical machines.

It is well recognized that the finite element method offers considerable advantage to the electrical machines analyst because it enables both intricate physical shapes and nonlinear properties to be represented [9]-[11]. The main disadvantage of the use of finite elements in machine analysis is that it usually involves the use of prodigious amounts of computer resources [12]. A FEM model that is developed for steady-state performance predictions may not be appropriate for transient analysis [13]. The suitability of the finite element method for the analysis of electrical machines has long been recognized, and a vast literature of published work now deals with the analysis of most types of machine.

The majority of the methods proposed by many researchers on the analysis of induction motors using FEM fall into two distinct categories, depending on how they deal with the rotor currents of the motor. One approach regards the rotor currents as a superposition of harmonic distributions, and writes voltage balance equations for each stator winding and each harmonic rotor distribution [14]-[20].

These equations are then solved to determine the unknown rotor currents using the finite element field analysis as a tool to calculate the circuit parameters, taking magnetic saturation into account. The alternative approach calculates the rotor currents directly as eddy currents induced in the rotor bars. Circuit equations are then written for the stator windings. These may be time stepped along with the field solution, or solved in the frequency domain using complex notation.

Both approaches have advantages and disadvantages. The superposition (circuit) approach is claimed to be faster and is inherently more capable of incorporating pole number dependent effects such as rotor skew. It does not include deep bar effect in the field solution, so that rotor bar resistance and slot leakage reactance must be modified after the field solution has taken place using correction factors, calculated using classical expressions, or otherwise.

The eddy current approach models the deep bar effect directly in the field equations, but requires longer time to run and cannot accommodate rotor skew without difficulty.

The two approaches also have much in common. Both employ two-dimensional field models, because the computing resource required for a full three-dimensional solution is still in the developing stage. Three-dimensional effects, such as end-winding and end-ring impedance are incorporated in an approximate manner, as is rotor skew. Both approaches dispense with the conventional equivalent circuit model for the induction motor, computing current, torque, input power and losses directly from the circuit or field equations.

The purpose of this paper is to present performance results obtained using the eddy current FEM approach for a three-phase induction motor for both no-load and full load conditions, and compare results so obtained to that predicted by the conventional constant parameter model.

THEORETICAL BACKGROUND

To determine the field distribution of an induction motor, a 2-dimensional transverse section spanning a pole pitch of the induction motor is represented. In reducing the problem to 2-dimensions, the following approximations are made, to account mainly for 3-dimensional effects:

- End effects due to flux fringing etc are treated by a modification of the stator core length.
- The laminated iron is represented by a suitable stacking factor which takes into account both the basic stacking effect and, where present, radial ventilation ducts.
- The rotor bar end-ring resistance is represented by modification of the rotor bar resistivity.
- Rotor speed is held constant at the required slip-frequency.

The transient magnetic field in terms of magnetic vector potential, A, the reluctivity, ν, conductivity, σ and current density, J, can be expressed as:

$$\frac{\partial}{\partial x}\left[\nu\frac{\partial A}{\partial x}\right]+\frac{\partial}{\partial y}\left[\nu\frac{\partial A}{\partial y}\right]=-J+\sigma\frac{\partial A}{\partial t} \quad (1)$$

where $\nu = f(A)$.

The term $\sigma \partial A/\partial t$ represents current induced in conducting material when flux changes with time. In some analysis of the induction motor, the flux and current time variations were assumed to be sinusoidal and the differential equation (1) become:

$$\frac{\partial}{\partial x}\left[\nu\frac{\partial A}{\partial x}\right]+\frac{\partial}{\partial y}\left[\nu\frac{\partial A}{\partial y}\right]=-J+j\omega\sigma A \quad (2)$$

However, this assumption requires the reluctivity to be constant throughout the time cycle, and therefore restricts the accuracy of the results. If information such as mmf harmonics, tooth pulsation harmonics and forces acting on the stator teeth are required, a full time stepping approach is needed.

The time stepping technique developed to solve equation (1) numerically was based on the finite element approach using a Newton-Raphson technique for rapid convergence at each time-step. The numerical equations were derived from Kirchhoff's current law applied at each node as described in [21], [22], also other techniques such as the energy approach or the Galerkin method could have been used. The resulting numerical form of the field equation (1) in matrix notation is:

$$[S](A)=\{I\}-[\Delta\sigma]\left[\frac{\partial A}{\partial t}\right] \quad (3)$$

where the terms of the matrix [S] and the vector {*I*} are:

$$S_{ij}=\frac{1}{4A_m}\left(\alpha_x q_i q_j+\alpha_y r_i r_j\right) \quad (4)$$

$$I_i = f_m \frac{A_m}{3} \quad (5)$$

A_m is the surface of the m-th finite element (m²) and $[\Delta\sigma]$ - is the conductivity matrix.

It can be observed that the terms S_{ij} depend only on the geometry and the material characteristics (expressed by the coefficients α_x and α_y). If the material is linear, the terms S_{ij} do not depend on the value of the potentials in the nodes (since α_x and α_y are constant with the field). By analogy, the terms I_i are only functions of the geometry of the element and of the forcing quantity f_m.

The magnetic nonlinearity of materials is allowed for by a predicator-corrector method using the Newton-Raphson algorithm to converge element permeabilities and node potentials to a consistent solution. The magnetic vector potential is predicted using a simple forward-difference time-stepping procedure whereby the potential from the previous time is related to that at the present time through $\partial A/\partial t$ at the previous time step as:

$$A_{t+\delta t} = A_t + \delta t \bullet \left[\frac{\partial A}{\partial t}\right]_t \quad (6)$$

impliedly,

$$\delta t = \frac{A_{t+\delta t} - A_t}{\partial A \,/\, \partial t} \quad (7)$$

An error vector $[E]$ of node currents is then formed by rearranging equation (3) as:

$$[E] = [S](A) - \{I\} + [\Delta\sigma]\left[\frac{\partial A}{\partial t}\right] \quad (8)$$

Thus the vector potential at the (j+i)th Newton-Raphson iteration at any time-step is corrected to:

$$\{A\}_{j+i} = \{A\}_j - \left[\frac{\partial A}{\partial t}\right]^{-1} [E] \quad (9)$$

The time-stepping is started numerically at t = 0 by assuming $\partial A/\partial t$ and A are zero. Using equations (3)-(9) the first Newton-Raphson iteration predicts the first estimate of the potential from which the flux and $\partial A/\partial t$ corresponding to the step change in current are evaluated. The induced emf and eddy currents can then be calculated at the start of the second nonlinear iteration to obtain a better estimate of the stator currents. The above procedure is repeated until errors in element permeablities and node potentials are below 10e-8.

MODEL FORMULATIONS OF THE MOTOR USING FEM METHOD

To solve the field problem of the induction motor under consideration, the values of the flux linkage per phase, ϕ in the j-th node of the m-th element, Φ_{mj} have to be computed in the nodes of each element. It is therefore necessary to prepare a system of equations, whose solution corresponds to the values of Φ_{mj}. To develop this system of equations, both the variational method and the residual method were adopted, but applied to each element separately.

$$R_i = \int_{\tau_D} W_i \left(L\phi^* - f \right) d\tau = 0 \quad (10)$$

where W_i is the i-th weighting function; R_i is the i-th residue; τ_D is the domain volume under consideration; L is a differential operator (e.g., Laplacian operator); ϕ is the unknown function to be determined and f is the forcing function.

In the case of Galerkin's method, equation (10) was applied to each element. The residual integral is put to zero. In the m-th element, the n integrals are given by:

$$R_{im} = \int_{\tau} v_i \left(L\phi_m^* - f_m \right) d\tau$$

$$R_{im} = \int_{\tau} v_i L \left(\sum_{j=1}^{N} \Phi_{mj} v_{mj} \right) d\tau - \int_{t} v_i f d\tau = 0$$

1 = 1, 2, 3, ..., n (11)

From equation (11) a system of n equations with the n unknown Φ_{mj} was obtained. Applying equation (11) to all the N_m elements that form the domain, and considering the relationships that link the adjacent elements, a system of this kind is obtained:

$$[SS][\phi] = [T] = 0 \quad (12)$$

which is formed by Nn equations, with Nn unknowns. Where $[SS]$ is the stiffness matrix; $[T]$ is the known terms matrix and $[\phi]$ is the column vector of the unknown coefficients ϕ_i.

However, using the variational method, the matrix [SS] is symmetrical, since the condition $\langle L\phi, \varphi \rangle = \langle \phi, L\varphi \rangle$ was satisfied.

FORMULATIONS FOR THE CONVENTIONAL CONSTANT PARAMETER MODEL (CCPM)

The equations of importance in the formulations of the CCPM model are equations (13) to (24).

$$Te = \frac{3}{2} \frac{P}{2\omega_b} \left[\psi_{ds} i_{qs} - \psi_{qs} i_{ds} \right] \quad (13)$$

Where Te - electromagnetic torque; ψ_{qs} - q-axis stator fl ux linkage; ψ_{ds} - d-axis rotor flux linkage; P - number of poles; i_{qs} - quadrature-axis stator current; i_{ds} - direct-axis stator voltage and ω_b - base angular velocity (rads/sec)

$$\frac{\omega e}{\omega b} = \frac{P}{2J\,\omega b} \int \left[T_e - T_l \right] dt \quad (14)$$

where J - moment of inertia of the motor: T_l - load torque and ω_e - electrical angular velocity of the rotor.

$$i_{qs} = \frac{\left(\psi_{qs} - \psi_{mq} \right)}{X_{sa}} \quad (15)$$

$$i_{ds} = \frac{\left(\psi_{ds} - \psi_{md} \right)}{X_{sa}} \quad (16)$$

$$i_{qr} = \frac{\left(\psi_{qr} - \psi_{mq} \right)}{X_{ra}} \quad (17)$$

$$i_{dr} = \frac{\left(\psi_{dr} - \psi_{md} \right)}{X_{ra}} \quad (18)$$

where ψ_{mq} - q-axis magnetizing flux linkage; ψ_{md} - d-axis magnetizing flux linkage; X_{sa} - stator phase leakage reactance; and X_{ra} - rotor phase leakage reactance.

$$\psi_{qs} = \omega_b \int \left[V_{qs} + \frac{r_s}{X_{sa}} \psi_{mq} - \frac{r_s}{X_{sa}} \psi_{qs} - \frac{\omega}{\omega_b} \psi_{ds} \right] dt \quad (19)$$

$$\psi_{ds} = \omega_b \int \left[V_{ds} + \frac{r_s}{X_{sa}} \psi_{md} - \frac{r_s}{X_{sa}} \psi_{ds} - \frac{\omega}{\omega_b} \psi_{qs} \right] dt \quad (20)$$

$$\psi_{qr} = \omega_b \int \left[V_{qr} + \frac{r_r}{X_{ra}} \psi_{mq} - \frac{r_r}{X_{ra}} \psi_{qr} - \frac{(\omega - \omega_e)}{\omega_b} \psi_{dr} \right] dt \quad (21)$$

$$\psi_{dr} = \omega_b \int \left[V_{dr} + \frac{r_r}{X_{ra}} \psi_{md} - \frac{r_r}{X_{ra}} \psi_{dr} - \frac{(\omega - \omega_e)}{\omega_b} \psi_{qr} \right] dt \quad (22)$$

where V_{qr} - quadrature-axis rotor voltage; V_{dr} - direct-axis rotor voltage; V_{qs} - quadrature-axis stator voltage; V_{ds} - direct-axis stator voltage; r_s - stator resistance/phase; and r_r - rotor resistance/phase.

$$\psi_{mq} = \left[\frac{1}{1 + X_{ra}/X_m + X_{ra}/X_{sa}} \right] \psi_{qr} + \left[\frac{1}{1 + X_{sa}/X_m + X_{sa}/X_{ra}} \right] \psi_{qs} \quad (23)$$

Similarly,

$$\psi_{md} = \left[\frac{1}{1 + X_{sa}/X_m + X_{sa}/X_{ra}} \right] \psi_{ds} + \left[\frac{1}{1 + X_{ra}/X_m + X_{ra}/X_{sa}} \right] \psi_{dr} \quad (24)$$

where X_m - magnetizing reactance of the machine.

OVERVIEW OF ANALYSIS

METHOD

The method used in this paper uses the eddy current finite element method to determine the components of the conventional equivalent circuit parameters for a given slip and applied voltage and to also predict the performance characteristics of the induction motor under test using Finite Element Method Magnetics (FEMM) software. This is performed using one-pole pitch section of both stator and rotor. The method may conveniently be explained by the following sequence of steps [10, 23]:

- Formulation of a finite element model of the motor under consideration
- Application of 3-phase currents to the stator windings models over a range of frequencies (The rotor currents are computed as induced eddy current, by the FEM software).
- For each analysis, the flux linkage of one phase of the machine will be evaluated to obtain the information that is required to fit the parameters in the circuit model.
- Performing a regression analysis to obtain the equivalent circuit parameter values.
- From the post processing result of the FEMM, the airgap flux densities at various excitation (stator) currents were obtained.
- Simulation of the motor on no-load leading to the determination of the back EMF of the motor/phase based on Fig.1 and equations (25) and (26).

Simulation of the motor under load condition using static mode, thus, the determination of the determination of the torque acting on the rotor.

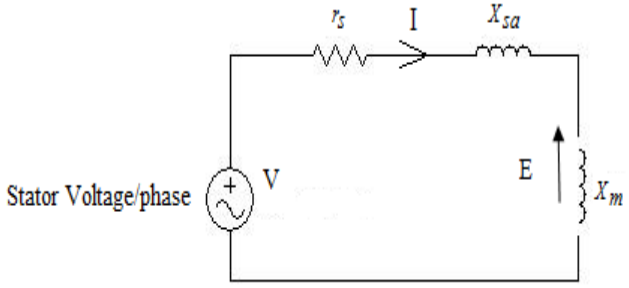

Fig. 1: Equivalent Circuit of Induction Motor on No-Load

$$E = V - I(r_S + jX_{sa}) \quad (25)$$

where, V- Phase voltage applied to the motor; E – Back EMF per phase induced in the motor; I – Stator current; r_S - Stator resistance per phase and X_{sa} - Stator leakage reactance.

The relationship between back EMF, E induced in a stator winding and the fundamental air-gap flux density can be presented as [10]:

$$E = \frac{2\pi f N_{ph} l d K_w B_g}{P} \quad (26)$$

where N_{ph} – No. of turn/phase; *d* – Mean air-gap diameter; *l* – Axial length of the motor; K_W winding factor; p – No. of poles; f – frequency; and B_g – Air-gap flux density.

For a star-connected stator winding, same as applied to the induction motor under test, the line-to-line induced voltage of the motor becomes $\sqrt{3}E$.

Table 1:Details of the motor

Motor type:	3-φ squirrel-cage Induction motor
Stator connection:	Star
Rated line voltage:	220V
Rated current:	2.40A
No-load current:	1.34A
Full-load torque:	5.4Nm
Rated speed:	1443 rpm
Frequency:	50 Hz
Number of poles:	4
Number of stator slots:	36
Number of rotor slots:	28
Stator bore diameter:	80.75 mm
Rotor diameter:	80 mm
Shaft diameter:	25 mm
Type of rotor cage:	Aluminium (grade 1100)
Machine length:	100 mm
Stator outside diameter:	130 mm
Air-gap length:	0.375 mm
Stator winding resistance:	4.4 Ω at 22°C
Rotor skew:	1 rotor slot pitch
Stator winding info:	44turns/slots
Lamination material:	0.5mm silicon iron core sheet
Moment of Inertia:	0.0012kg-m^2

RESULTS

The procedure outlined above was verified by comparing FEM results with results obtained from a conventional constant parameter model (CCPM) on a 220V, 2Hp, 4-pole cage induction motor. The stator and rotor laminations for this motor are shown in Fig. 2, and other details are summarised in Table 1.

Comparison of results

The no-load and load performance characteristics obtained using both the described FEM and CCPM are compared to the operating point's data supplied by the manufacturer of the induction motor under test as shown in Table 2.

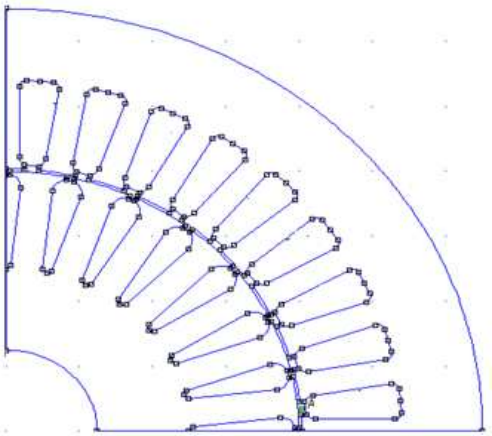

Fig. 2: One pole-pitch section of the motor

The open-circuit and dynamic performance characteristics of the induction motor obtained using FEM are as shown in Figs 3 to 5.

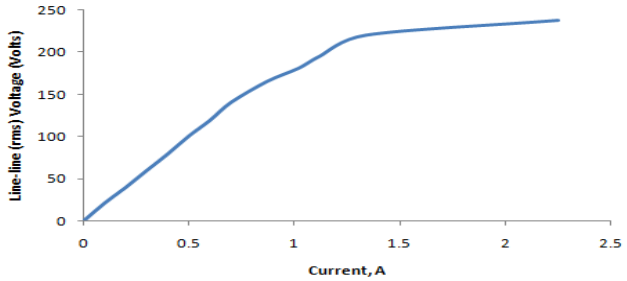

Fig. 3: No-load (open-circuit) characteristic of the induction motor

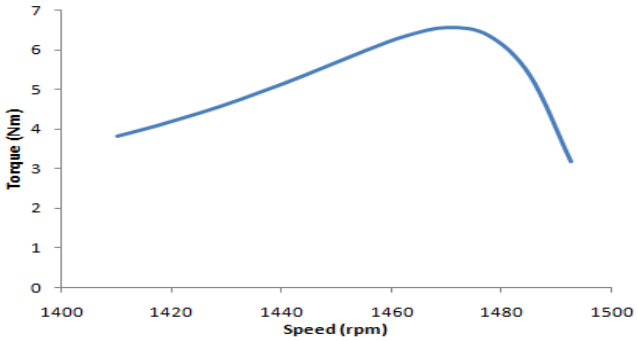

Fig. 4: Torque-speed characteristic of the induction motor on load using FEM Version 4.0

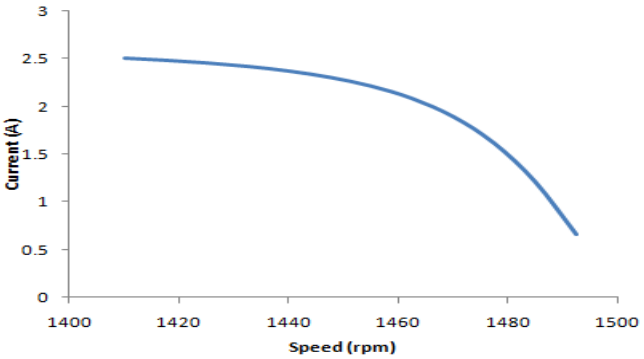

Fig. 5: Current-speed characteristics of the induction motor on load using FEMM

The simulation results obtained from the CCPM on no-load are shown in Figs. 6 and 7.

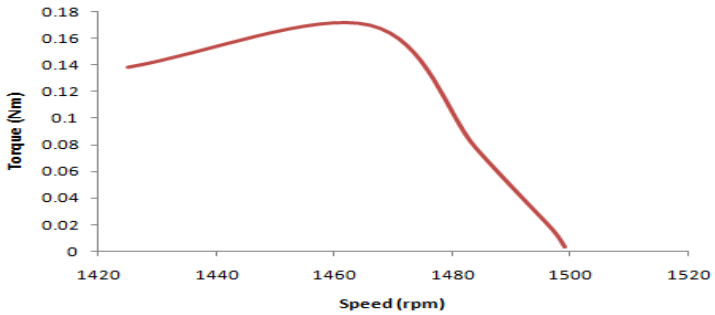

Fig. 6: Torque-speed characteristics of the motor on no-load using CCPM

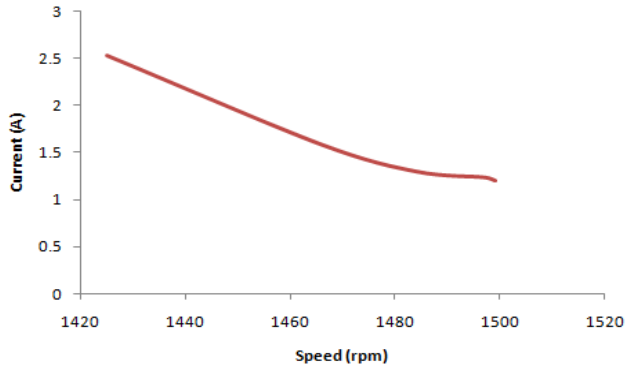

Fig. 7: Current-speed characteristics of the motor on no-load using CCPM

The simulation results obtained from the CCPM on load are shown in Figs. 8 and 9

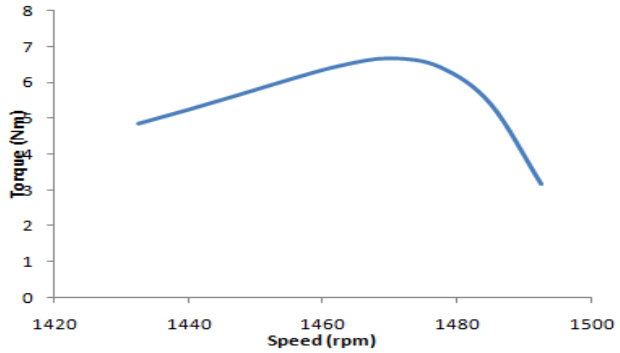

Fig. 8: Torque-speed characteristics of the motor on load using CCPM

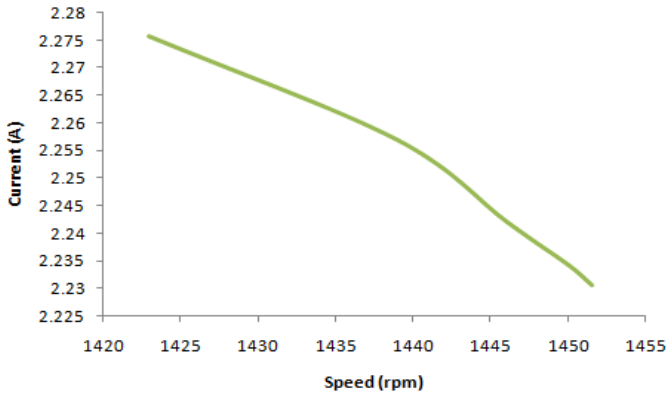

Fig. 9: Current-speed characteristics of the motor on load using CCPM

Table 2: Results comparison

	FEM	CCPM	Manufacturer's data
No-load current (A)	1.34	1.21	1.34
Full-load current (A)	2.34	2.25	2.40
Full-load torque (Nm)	5.399	5.6	5.4

The predictions made at the operating points, using the FEM analysis are seen to be in good agreement with manufacturer's data with the exception of the full-load current. The disparity between the full load currents corresponding to rated voltage predicted by both the FEM and the manufacturer is caused by the following factors, which were assumed in the FEM analysis. Among the issues that have been neglected in the analysis are the rotor skewness and harmonic effects. Even though, the predictions from the CCPM are also good, their accuracy is not as good as that obtained from the FEM analysis. A perplexing problem concerning the CCPM is that it predicted the value of the electromagnetic torque to be higher than manufacturer's value and also its current predictions are lower than that given by the manufacturer.

CONCLUSION

Combined stator and rotor models were used in the FEM analysis, consisting of the minimum representative part (one pole pitch) of both the stator and rotor. The method gave good results for the four-pole motor. The advantages claimed by this FEM analysis approach are:

- The use of magneto static conditions in the analysis, thereby making the field solution to be simplified.
- The method makes use of 2D-Finite Element software as against 3D-Finite Element software, such that the complexity of the field equations and the solution time are reduced.
- The FEM-circuit approach enabled the desired performance characteristics of the induction motor (current and torque) to be predicted in a simple manner.

REFERENCES

1. Ho, S.L., Fu, W.N., and Wong, H.C., "Application of Automatic Choice of Step Size for Time Stepping Finite Element Method to Induction Motors", IEEE Trans. Magnetics, Vol. 33, No. 2, pp. 1370-1373, March 2001.
2. Vassent, E., Meunier, G., et al, "Simulation of Induction Machine Operation Using a step by step Finite Element Method Coupled with Circuits and Mechanical Equations", IEEE Trans. on Magnetics, Vol. 27, No. 6, pp. 5232-5234, Nov. 1991.
3. Demerdash, N.A., Bangura, J.F. and Arkadan, A.A., "A Time-Stepping Coupled Finite Element State Space Model for Induction Motor Drives, I. Model Formulation and Machine Parameter Computation", IEEE Trans. Energy Conversion, Vol. 14, pp. 1465-1471, 2007.
4. Faiz, J.B., Ebrahimi, M. and Sharifian, M.B.B., "Finite Element Transient Analysis of an On-Load Three Phase Squirrel-Cage Induction Motor with Static Eccentricity", Journal of Electromag., Vol. 27, pp. 543-569, 2007.
5. Fiser, R., "Application of a Finite Element Method to Predict Damage Induction Motor Performance", IEEE Trans. Magnetics, Vol. 37, pp. 3635-3639, 2001.
6. Salon, S.J., Burow, D.W., et al., "Finite Element Analysis of Induction Machines in the Frequency Domain", IEEE Trans. Magnetics, Vol. 29, pp. 1438-1441, 1993.
7. Chari, M.V.K., "Finite Element Analysis of Electrical Machinery and Devices", IEEE Trans. on Magnetics,Vol., MAG-16, No. 5, pp. 1014-1018, September 1990.
8. Salon, S.J., "Finite Element Analysis of Electric Machinery", IEEE Computer Applications in Power, pp. 29-32, April 2006.
9. Lowther, D.A. and Silvester, P.P., *Computer-Aided Design in Magnetics*, Springer-Verlag, 1985.
10. Bianchi, N., Bolognani, S. and Comelato, G., "Finite Element Analysis of Three Phase Induction Motors: Comparison of Two Different Approaches", IEEE Trans. on Energy Conversion, Vol. 14, No. 4, pp. 1523-1528, December 1999.
11. Williamson, S. and Gersh, D.R., "Finite Element Calculation of Double-Cage Rotor Equivalent Circuit Parameters", IEEE Trans. on Energy Conversion, Vol. 11, No. 1, pp. 41-48, 2006.
12. Hughes, T.J.R., Linear Static and Dynamic Finite Element Analysis, Dover Publications, Mineola, 2000.
13. Belmans, R., Findlay, R.R.D. and Geysen, W., "A Circuit Approach to Finite Element Analysis of a Double Squirrel-Cage Induction Motor", IEEE Trans. on Energy Conversion, Vol. 5 No. 6, pp. 719-724, 1990.
14. Williamson, S. and Ralph, J.W., "Finite-Element Analysis for an Induction Motor Fed from a Constant Voltage Source", IEE Proc-B, pp. 18-24, 1983.
15. Williamson, S. and Begg, M.C., "Analysis of Cage Induction Motors- A Combined Fields and Circuits Approach", IEEE Trans. MAG-21, Vol.6, pp. 2396-2399, 2005.
16. Williamson, S., Smith, A.C., Begg, M.C. and Smith, J.R., "General Techniques for the Analysis of Rotating Induction Machines Using Finite Elements", Proc. Intl. Conf. Evolution and Modern Aspects of Induction Machines, Turin, pp. 389-395, 1986.
17. Williamson, S., Lim, L.H. and Smith, A.C., "Transient Analysis of Cage Induction Motors Using Finite Elements", IEEE Trans. MAG-26, Vol.2, pp. 941-944, 1990.
18. Williamson, S., Lim, L.H. and Robinson, M.J., "Finite-Element Models for Cage Induction Motor Analysis", IEEE Trans. Industry Apps., Vol. 26, No. 6 pp. 1007-1017, Nov/Dec, 1990.
19. Smith, A.C., Williamson, S., and Smith, J.R., "Transient Currents and Torques in Wound-Rotor Induction Motors Using the Finite Method", IEE Proc. B, Vol. 137, No. 3, pp. 160-173, 1999.
20. Mukherjee, S., Adams, G.E. and Hoft, R.G., "FEM Analysis of Inverter-Induction Motor Rotor Conduction Losses", IEEE Trans., Energy Conversion, Vol.4, No.4, pp. 671-680, 1989.
21. Hannalla, A.Y and McDonald, D.C., "Numerical Analysis of Transient Field Problems in Electrical Machines", Proc. IEE, Vol. 123, pp. 893-898, 2007.
22. Turner, P.J., "Finite Element Simulation of Turbine-Generator Terminal Faults and Application to Machine Parameter Prediction", IEEE Trans. PAS, Winter meeting, 1986.
23. http://femm.com accessed on the 15th April, 2012.